Establishing a degree of order: obtaining high-resolution NMR structures from molecular alignment

Nico Tjandra

Address: Laboratory of Biophysical Chemistry, National Heart, Lung, and Blood Institute, National Institutes of Health, 9000 Rockville Pike, Bethesda, MD 20892-0380, USA.

E-mail: nico@helix.nih.gov

Structure September 1999, 7:R205–R211
http://biomednet.com/elecref/09692126007R0205

0969-2126/99/$ – see front matter

X-ray crystallography and high-resolution nuclear magnetic resonance (NMR) provide the two main tools for determination of the three-dimensional structure of biomolecules. In contrast to X-ray crystallography, where one observes the electron density of the molecule in three-dimensional space, high-resolution NMR only provides access to local information in the form of short distances (less than 5 Å) and dihedral angles [1,2]. Distances are typically obtained from the relaxation phenomena between a pair of protons, whereas dihedral angles are derived from the scalar (J) coupling between two nuclei that are connected by more than one chemical bond. From the compilation of the local structural information the three-dimensional structure of the molecule can be constructed. This method is possible provided a large and redundant collection of these local constraints is available. What is missing from NMR structural information is a way to directly link different structural elements that are not in proximity. For small globular and compact proteins this deficiency is not debilitating. One can describe structural features on opposing sides of the molecule through their relative position with respect to the core of the protein, where typically a large number of distance constraints can be measured. In nonglobular entities, however, this deficiency becomes an important limiting factor to determining the correct structure of the molecule. For instance, in multidomain proteins and protein–protein or protein–nucleotide complexes, typically one is limited to observing short distance information at the linker of the modules or at the interface of the complex, respectively. A proper positioning of the structural components requires these short distances to be extremely accurate. This is a tough requirement, considering the quality of the data for the typical size of molecules being studied, as well as the complex nature of the interaction that is probed to extract distance information in solution NMR. Furthermore, the number of distance constraints observed in these regions is often small, thus compounding the difficulty. In the case of RNA or DNA, this problem arises plainly due to the lack of observable distance information. The relatively large number of degrees of freedom also complicates the problem and nucleotide structures cannot therefore usually be well defined.

The strong magnetic nuclear–nuclear and nuclear–electron interactions within a molecule contain vital structural information. Brownian rotation of the molecules in solution averages all of these interactions. This allows solution NMR to take advantage of the resultant sharp resonance lines and to utilize a somewhat simpler interpretation of the data to simultaneously study the whole structure of the biomolecule. Solid-state NMR, however, has long enjoyed the availability of those same interactions, due to the absence of fast random rotation of the molecule, to provide a great deal of structural information. In order to avoid complicated interpretation of the data in solids, studies have mainly focused on relatively small molecules or a specific part of a large molecule. Naturally, an ideal solution for high-resolution NMR is to find a compromise in which these strong interactions could be observed without jeopardizing the excellent solution NMR properties. The only way to reintroduce these strong interactions is to bias their fast rotational averaging in solution. One way to accomplish this is to align the molecule in solution.

Alignment of molecules in solution

There are several ways that a net alignment of biomolecules in solution can be achieved. A small degree of alignment can be observed for biomolecules with non-zero magnetic susceptibility anisotropy when they are placed in a strong magnetic field [3–5]. This is analogous to putting a small bar magnet in a strong magnetic field. In general these molecules would have a degree of alignment in the order of 10^{-5}–10^{-4}. That is to say that there is 10^{-5}–10^{-4} more likelihood of one molecule being found in a preferred orientation. For instance, a typical diamagnetic molecule, such as a protein, would have an expected susceptibility anisotropy in the order of $2–4 \times 10^{-34}$ m^3/molecule [5]; this would provide a net order of alignment of 10^{-5}. Only in favorable cases where the alignment is large enough can one measure the magnetic interactions and use this information for structure determination. This narrows the application of this method to paramagnetic molecules where the paramagnetic center dominates the susceptibility [3,6], and nucleotides where the regular base stacking results in a relatively large susceptibility anisotropy [4,7]. Both of these cases increase the alignment by one order of magnitude relative to the diamagnetic counterpart. In addition to the limitation of the applicability of this method to specific systems, the alignment can only be observed in the presence of a very strong magnetic field.

An alternative way of producing a slight alignment of the macromolecule is by adding aqueous liquid crystalline phase to the system [8]. Liquid crystal molecules, due to their susceptibility anisotropy, will cooperatively orient themselves in a magnetic field. In turn, the biomolecule under study will interact with the liquid crystal resulting in a net alignment. The general applicability of this method to different biological systems and the lack of a requirement for a very high magnetic field are just a few of its advantages. Currently there are two different classes of media that are used for this purpose; classification is made on the basis of the shapes of the molecules that make up these media. The first class contains large disc particles. One example of this media comprises a mixture of lipids containing dimyristoyl phosphatidylcholine (DMPC) and various detergents that will undergo a phase transition at slightly above room temperature to form large discs called bicelles [9,10]. A second example is the use of purple membrane that stays as a large two-dimensional array in solution [11,12]. Figure 1a illustrates the organization of these lipid-based molecules and the protein in the system. The second class of media consists of large rod molecules the system arrangement of which is depicted in Figure 1b. These long rods are viral particles. A suspension of filamentous bacteriophage Pf1 [13], fd, and tobacco mosaic virus [14] are just some examples of this class of media that have been shown to induce alignment of biomolecules. Not all of these media are liquid crystals by definition. Purple membrane creates order without undergoing phase transition or requiring local cooperativity [11]. Besides their shapes these classes of molecules also have other distinct properties. Lipid bicelles can be made up of charged as well as neutral lipids [15,16], whereas the purple membrane [11,12] and all of the viral particles are electrically charged [13,14]. Lipid bicelles undergo liquid crystal phase transition over a relatively small range of temperature in contrast to the other types of media. By varying the content of the lipid mixture, however, one can still shift this temperature range [15]. One thing that all of these molecules have in common is the ability to induce order in the system at relatively low concentrations. This is important to avoid space restrictions that can hamper the rotational tumbling of the biomolecule of interest and will subsequently result in broadening of its resonance lines.

There are additional advantages of this method over the magnetic field alignment. The liquid crystal method typically creates an alignment that is at least one order of magnitude larger than the field alignment. Furthermore, the alignment by liquid crystal can be tuned. The magnitude as well as the direction of the alignment can be adjusted by various means depending on the interaction between the biomolecule and the liquid crystal. Even though the nature of the interaction is still under debate, some recent results suggest that when the neutral liquid crystal phase is used the major component of the interaction is steric [17], and when the liquid crystal is charged the electrostatic interaction can have a substantial contribution [16]. By changing the concentration of the liquid crystal one can adjust the magnitude of the alignment [15]. Changing the temperature of lipid bicelle media within its liquid crystal range will also attenuate the alignment, although the effect is much smaller than that obtained by varying the concentration [15]. Varying the electrostatic interaction when its contribution is relevant can change the direction as well as the magnitude of the alignment. This can be achieved by

Figure 1

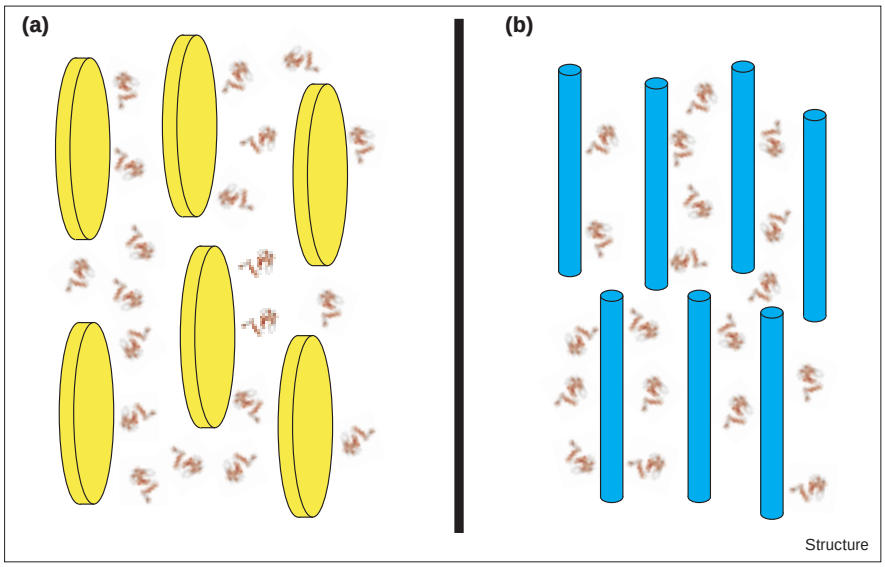

Cartoon illustrations of the two different classes of liquid crystal media. (a) The large disc particles represent lipid bicelles or the purple membrane. (b) The long rods represent viral particles. The bicelles orient with their normal orthogonal to the magnetic field [8]. In contrast, the long phage particles align with their long axis parallel to the field [13].

doping the neutral bicelles with charged lipids [16], varying the concentration of counter ions in the solution [12], or by the incorporation of a fusion tag on the biomolecule of interest [16]. All of these factors make the use of liquid crystals to induce alignment very attractive.

Measurable quantities in aligned molecules

A slight alignment of the biomolecule allows many physical quantities that were only common to solid-state NMR to now also be available for high-resolution NMR. These quantities include dipolar coupling, chemical-shift anisotropy (CSA), and quadrupolar coupling, to mention just a few. Because CSA is not averaged to zero by the molecular rotation, small changes of the orientation-induced isotropic chemical shift can be observed [18,19]. As the changes in the chemical shifts are relatively small, however, the information on the CSA can only be extracted by careful analysis. Due to the size of the observed CSA values and the current lack of understanding of structural effects that contribute to them, their use for structural determination in high-resolution NMR is presently very limited. The use of alignment-induced residual quadrupolar coupling for structure determination is limited to small molecules, because the property of quadrupolar relaxation does not favor large biomolecules. On the other hand, residual dipolar coupling has become the main choice to extract structural information through alignment of the molecule due to its substantial size and more favorable dipolar relaxation property.

A general method for measuring these quantities is to compare the observed values in the isotropic (non-aligned) versus the aligned state. In the case of CSA, the difference between the observed chemical shifts provide information on the alignment as well as the CSA tensor [18,19]. In the case of the quadrupolar coupling, a non-zero splitting of the quadrupolar resonance in the aligned molecule can be observed [20]. The size of the splitting is a measure of the alignment of the molecule as well as the size of the electric field gradient at the nucleus. Dipolar coupling is reintroduced in the aligned molecule as a change in the apparent scalar (J) coupling of the interacting magnetic nuclei. Thus, by measuring the scalar coupling in the isotropic condition one can determine the J value, and subtracting that from the value measured in a liquid crystal medium yields the residual dipolar coupling (D) [8]. Figure 2 shows two-dimensional correlation plots between amide ^{1}H and ^{15}N for human G_{α} interacting protein (GAIP) in the isotropic and liquid crystal medium. The distance in hertz between the resonance doublets in the isotropic medium represents the J coupling, while in the liquid crystal medium it equals the sum of J and the residual dipolar coupling (J + D).

Structure determination of aligned molecules

The dipolar coupling of two interacting magnetic nuclei depends on the distance between them, their gyromagnetic ratios, and the orientation of the interaction vector with respect to the magnetic field. When the molecule is aligned, there is a fixed orientation between the molecule and the applied magnetic field and a simple transformation can be done to describe the residual dipolar coupling in the alignment coordinate system. Furthermore, as the alignment is not static, but rather an average over a distribution of orientations of molecules in the system, a proper statistical averaging of the expected residual dipolar coupling can be carried out [3]. All these steps produce a general expression for the residual dipolar coupling which can be written as [8]

$$D_{pq} \propto -\mathbf{S}\,\gamma_p\gamma_q\,[A_a\,(3\cos^2\theta - 1) + 3/2\,A_r\,(\sin^2\theta\,\cos 2\varphi)] / r^3_{pq} \qquad (1)$$

where $\mathbf{S}$ is the generalized order parameter of the interaction vector, γ_p and γ_q are the gyromagnetic ratios of the

Figure 2

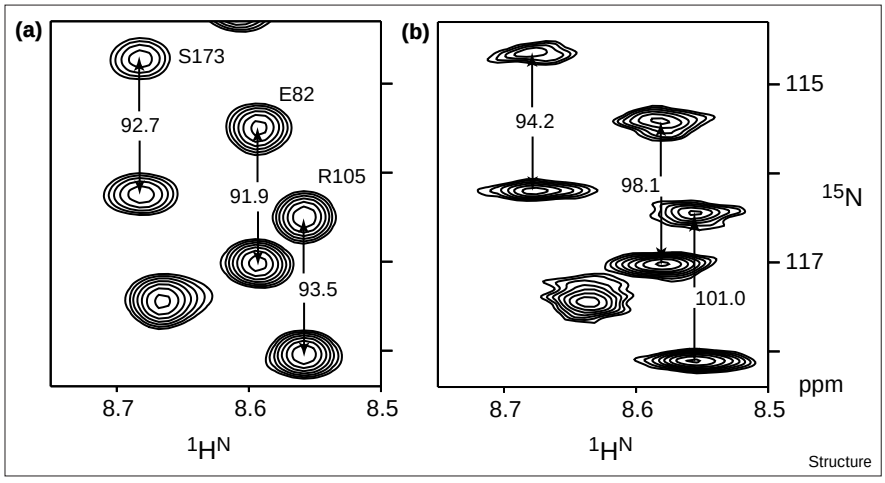

Plots of two-dimensional correlation ^{1}H and ^{15}N spectra for human GAIP in (a) an isotropic condition and (b) a liquid crystal medium containing 3% (w/v) of a 3:1 molar ratio of DMPC:dihexanoyl phosphatidylcholine (DHPC). A resonance doublet is observed for each pair of ^{1}H–^{15}N nuclei. The measured apparent scalar couplings are noted in hertz. The broadening of the $^{1}H^{N}$ resonances of human GAIP in the liquid crystal medium is due to long-range ^{1}H–^{1}H dipolar couplings.

Figure 3

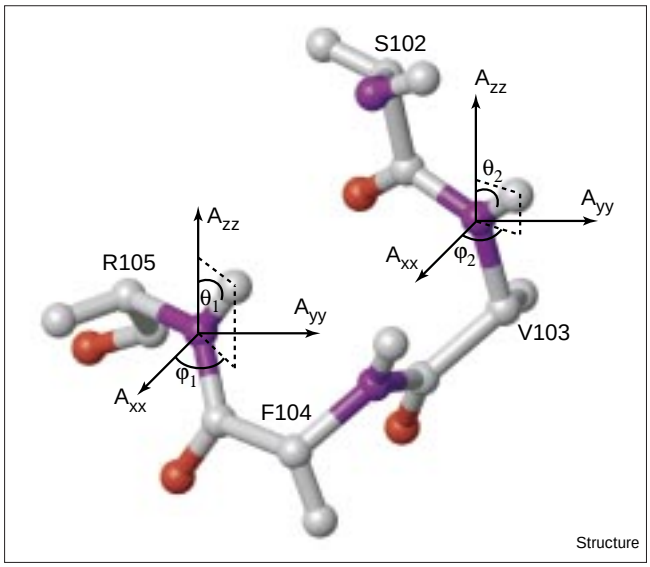

Orientation of the dipolar interaction vectors between $^1H^N$ and ^{15}N nuclei of four residues of GAIP in the alignment coordinate system. For this pair of nuclei the interaction vector coincides with the chemical bond connecting them. The single axis system of the alignment tensor, to which all interaction vectors are referenced, is designated as A_{xx}, A_{yy} and A_{zz}. The angles θ_M and φ_M describe the orientation of the interaction vector M in the common alignment frame. For clarity, the reference coordinate system is only drawn for two of the residues. (The figure was generated using the program MOLMOL [27].)

Figure 4

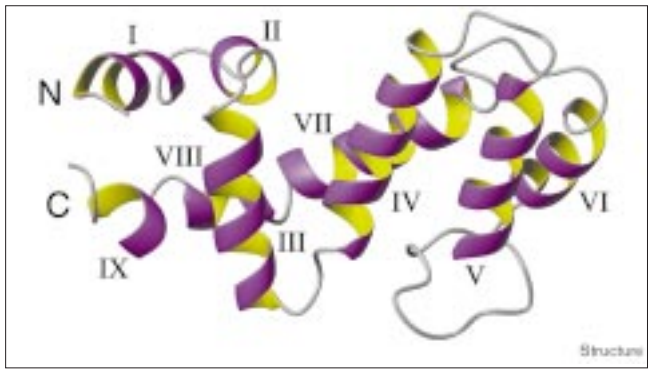

A ribbon diagram depicting the backbone of the lowest energy structure of human GAIP. (The figure was generated using the program MOLMOL [27].)

nuclei, and r_{pq} is the distance between them. The angles θ and φ describe the orientation of the vector between the two nuclei in the coordinate system of the alignment tensor **A**. For a system containing a given liquid crystal medium there should only be one alignment tensor. Therefore, all of the measured dipolar couplings provide information on angular orientations of the interaction vectors to one reference frame. Figure 3 illustrates how the angles θ and φ define the orientation of the interaction vectors in the common frame. As all of the vectors are defined within the same reference frame, one essentially obtains the relative orientation of these vectors in a three-dimensional space which is independent of the distance separating them. The magnitude of the alignment tensor can be described by two values, A_a and A_r, which are the axial and rhombic component, respectively. The variation of **S** for a well-defined structure is small, therefore the average value of **S** can safely be absorbed into the apparent alignment magnitude $\mathbf{S}A_a$ and $\mathbf{S}A_r$ [8]. This would leave one with $\mathbf{S}A_a$, $\mathbf{S}A_r$, the distance between the two nuclei, and the direction of alignment as unknowns. If one concentrates on measuring only residual dipolar couplings for directly bonded nuclei, then the distance dependence of the dipolar coupling is eliminated. A method for estimating the apparent size of the alignment magnitude $\mathbf{S}A_a$ and $\mathbf{S}A_r$ by inspection of the distribution of the measured dipolar couplings has been proposed recently [21], thus leaving the direction of the alignment as the only unknown. There are several different methods of deducing the orientation of the alignment tensor. If the structure of the whole molecule or part of it is known then a global fitting of the observed dipolar couplings to the structure will yield the orientation of the tensor [5]. In the case where the structure of the molecule is yet to be determined then the dipolar coupling data can be included during the structure calculation [7]. During the calculation, a continuous fitting of the dipolar coupling values to the molecule with respect to one reference axis system, which is allowed to float, is carried out. This is achieved by incorporating a harmonic energy term, which is related to the difference between calculated and measured dipolar couplings, in the calculation. At the end of the calculation the structure produced should satisfy all of the measured dipolar couplings to a reference axis system that represents the direction of the alignment tensor.

The precision and accuracy of NMR structures improve with the addition of dipolar coupling

Human GAIP [22], a member of a novel family of regulators of G-protein signaling (RGS), was chosen as an example to illustrate the use of dipolar coupling for structure determination. GAIP is a 217-residue protein that contains one RGS domain which is responsible for its G_α interaction [22]. The solution structure of the 128-residue core of GAIP was recently published with a backbone precision of 0.46 Å [23]. The protein contains nine α helices making up two different domains. The first domain contains helices I, II, III, VIII and IX; a four-helix bundle containing helices IV, V, VI and VII forms the second domain. Helix numbering follows their order from the N to the C terminus. To illustrate the relative positioning of these helices within the structure a ribbon

Figure 5

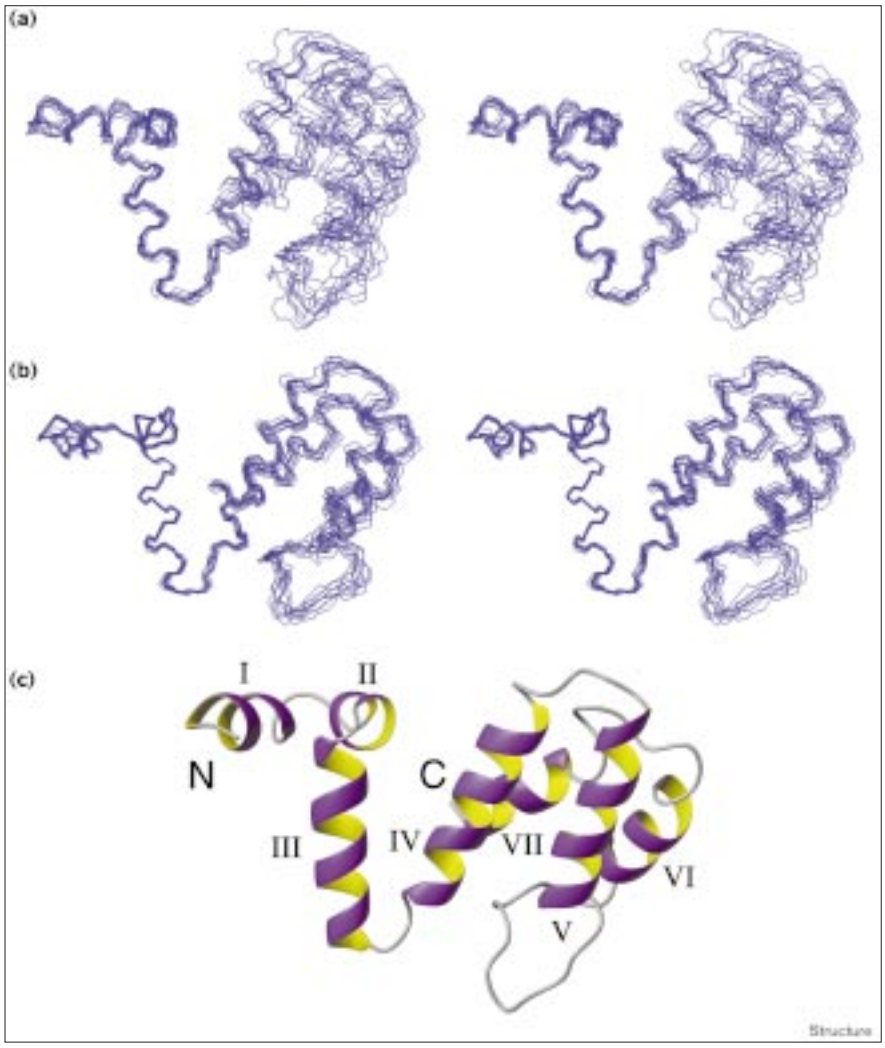

Stereoview superposition of ten NMR structures calculated for the truncated GAIP (a) without and (b) with dipolar couplings. All structures are superimposed based on the backbone atoms of the N-terminal domain containing helices I, II and III. (c) A ribbon representation of the backbone of the minimized average structure of truncated GAIP calculated with dipolar couplings. (The figure was generated using the program MOLMOL [27].)

representation of GAIP is shown in Figure 4. The relative orientation between the two domains is defined by contacts between helices II, III, IV, VII and VIII. For the purpose of illustrating the long-range nature of residual dipolar coupling, helices VIII and IX were deleted from the structure. The resulting structure will be referred to as truncated GAIP and corresponds to a removal of 22 residues from the C terminus. This deletion was done for one obvious reason, to reduce the number of contacts defining the relative orientations between the two domains. After deletion of these helices the relative domain orientation is defined with only contacts between helices II, III and IV. In this configuration the total number of observable nuclear Overhauser effect (NOE) contacts is 39 and cover a total of 847 $Å^2$ surface area. The number of NOE contacts for the given surface area is representative of a typical number expected for a protein–DNA complex [24,25].

Distance constraints that were incorporated in the structure calculations for the truncated GAIP include 849 interresidue and 213 intraresidue NOE constraints, as well as 32 hydrogen-bond constraints for the regular secondary structure elements. In addition, a total of 67 and 66 dihedral constraints for φ and ψ backbone angles were used, respectively. Four different families of dipolar couplings were measured for truncated GAIP: 52 D_{NH}, 53 $D_{C\alpha C'}$, 34 $D_{C\alpha H}$, and 52 $D_{C'N}$. A total of 50 structures were each calculated with and without the inclusion of the dipolar couplings. The calculations were performed in a similar fashion to those described previously [23]. The ten lowest energy structures from each family are plotted in Figure 5. These structures were superimposed based on the backbone atoms of helices I, II and III. A ribbon representation of the minimized average structure of the family calculated with dipolar couplings is also shown (Figure 5) to present a clearer picture for the orientation of the helices.

Upon the addition of the dipolar couplings, a substantial increase in the precision of the structures can be observed. The backbone root mean square deviation (rmsd) values calculated for the two families of structures including only helices I, II and III are 0.29 and 0.53 Å for the ones calculated with and without dipolar couplings, respectively. The heavy atom rmsd value also decreases from 1.07 to 0.90 Å after the inclusion of the dipolar couplings. The same trend is observed when the rmsd values are calculated for only helices IV, V, VI and VII. This shows that the precision of the individual domain improves substantially. More importantly, as can be seen in Figure 5, the relative orientation of the two domains is much better defined when the dipolar coupling data were included. Backbone rmsd values for the C-terminal four-helix bundle are 1.10 and 2.39 Å for structures calculated with and without dipolar couplings, respectively. The rmsd for the four-helix bundle was calculated by superimposing the structures based only on the backbone atoms of helices I, II and III, as depicted in Figure 5. In addition to the improved precision, the accuracy of the calculated structures also increases upon the addition of dipolar couplings. The rms shift between the average structure calculated without the dipolar couplings and the average structure of the full GAIP is 1.45 Å; a similar comparison using the average structure calculated with the dipolar couplings yields a pairwise rms of 0.46 Å. These calculations were done only for helices I, II and III. The values suggest that the deletion of helices VIII and IX had a detrimental effect on the core of the first domain, but also imply that the dipolar couplings were able to recover the relative orientations of these first three helices. The improvements described here were obtained by the introduction of a relatively small number of dipolar couplings, considering the total number of residues in the protein.

Future directions

The application of molecular alignment is not limited only to relatively small (less than 25 kDa) biomolecules. In fact, the use of dipolar coupling data will have a very important role in determining the structure of large molecules by NMR. The high incorporation of deuterium is the most common avenue taken to solve the structure of large (greater than 25 kDa) molecules by NMR [26]. In addition to improving the relaxation property of the system, the incorporation of deuterium also reduces the complexity of data interpretation by lessening the number of observable protons, thus substantially decreasing the number of distance constraints that can be measured. The accumulation of error in defining a large molecule using local structural information can be alleviated by use of the long-range information that dipolar coupling can provide.

In summary, the precision and accuracy of NMR structures are increased when data obtained from molecular alignment methods are used. This will most certainly result in the constant improvement of this methodology and its application towards structure determination by high-resolution NMR.

Acknowledgements

I would like to thank Eva de Alba for providing structural data as well as Ad Bax and James Baber for their critical comments.

References

1. Wüthrich, K. (1986). *NMR of Proteins and Nucleic Acids.* John Wiley & Sons, New York, NY.
2. Clore, G.M. & Gronenborn, A.M. (1989). Determination of 3-dimensional structures of proteins and nucleic-acids in solution by nuclear magnetic-resonance spectroscopy. *Crit. Rev. Biochem. Mol. Biol.* 24, 479-564.
3. Tolman, J.R., Flanagan, J.M., Kennedy, M.A. & Prestegard, J.H. (1995). Nuclear magnetic dipole interactions in field-oriented proteins – information for structure determination in solution. *Proc. Natl Acad. Sci. USA* 92, 9279-9283.
4. Kung, H.C., Wang, K.Y., Goljer, I. & Bolton, P.H. (1995). Magnetic alignment of duplex and quadruplex DNAs. *J. Magn. Reson. B* 109, 323-325.
5. Tjandra, N., Grzesiek, S. & Bax, A. (1996). Magnetic field dependence of nitrogen-proton J splittings in ^{15}N-enriched human ubiquitin resulting from relaxation interference and residual dipolar coupling. *J. Am. Chem. Soc.* 118, 6264-6272.
6. Beger, R.D., Marathias, V.M., Volkman, B.F. & Bolton, P.H. (1998). Determination of internuclear angles of DNA using paramagnetic assisted magnetic alignment. *J. Magn. Reson.* 135, 256-259.
7. Tjandra, N., Omichinski, J.G., Gronenborn, A.M., Clore, G.M. & Bax, A. (1997). Use of dipolar ^{1}H–^{15}N and ^{1}H–^{13}C couplings in the structure determination of magnetically oriented macromolecules in solution. *Nat. Struct. Biol.* 4, 732-738.
8. Tjandra, N. & Bax, A. (1997). Direct measurement of distances and angles in biomolecules by NMR in a dilute liquid crystalline medium. *Science* 278, 1111-1114.
9. Sanders, C.R. & Schwonek, J.P. (1992). Characterization of magnetically orientable bilayers in mixtures of dihexanoylphosphatidylcholine and dimyristoylphosphatidylcholine by solid-state NMR. *Biochemistry* 31, 8898-8905.
10. Sanders, C.R., Hare, B.J., Howard, K.P. & Prestegard, J.H. (1994). Magnetically-oriented phospholipid micelles as a tool for the study of membrane-associated molecules. *Prog. Nucl. Magn. Reson. Spect.* 26, 421-444.
11. Koenig, B.W., Hu, J.S., Ottiger, M., Bose, S., Hendler, R.W. & Bax, A. (1999). NMR measurement of dipolar couplings in proteins aligned by transient binding to purple membrane fragments. *J. Am. Chem. Soc.* 121, 1385-1386.
12. Sass, J., *et al.*, & Grzesiek, S. (1999). Purple membrane induced alignment of biological macromolecules in the magnetic field. *J. Am. Chem. Soc.* 121, 2047-2055.
13. Hansen, M.R., Mueller, L. & Pardi, A. (1998). Tunable alignment of macromolecules by filamentous phage yields dipolar coupling interactions. *Nat. Struct. Biol.* 5, 1065-1074.
14. Clore, G.M., Starich, M.R. & Gronenborn, A.M. (1998). Measurement of residual dipolar couplings of macromolecules aligned in the nematic phase of a colloidal suspension of rod-shaped viruses. *J. Am. Chem. Soc.* 120, 10571-10572.
15. Ottiger, M. & Bax, A. (1998). Characterization of magnetically oriented phospholipid micelles for measurement of dipolar couplings in macromolecules. *J. Biomol. NMR* 12, 361-372.
16. Ramirez, B.E. & Bax, A. (1998). Modulation of the alignment tensor of macromolecules dissolved in a dilute liquid crystalline medium. *J. Am. Chem. Soc.* 120, 9106-9107.
17. de Alba, E., Baber, J.L. & Tjandra, N. (1999). The use of residual dipolar coupling in concert with backbone relaxation rates to identify conformational exchange by NMR. *J. Am. Chem. Soc.* 121, 4282-4283.
18. Ottiger, M., Tjandra, N. & Bax, A. (1997). Magnetic field dependent amide ^{15}N chemical shifts in a protein–DNA complex resulting from magnetic ordering in solution. *J. Am. Chem. Soc.* 119, 9825-9830.

19. Cornilescu, G., Marquardt, J.L., Ottiger, M. & Bax, A. (1998). Validation of protein structure from anisotropic carbonyl chemical shifts in a dilute liquid crystalline phase. *J. Am. Chem. Soc.* **120**, 6836-6837.
20. Prestegard, J.H., Miner, V.W. & Tyrell, P.M. (1983). Deuterium NMR as a structural probe for micelle-associated carbohydrates: D-mannose. *Proc. Natl Acad. Sci. USA* **80**, 7192-7196.
21. Clore, G.M., Gronenborn, A.M. & Bax, A. (1998). A robust method for determining the magnitude of the fully asymmetric alignment tensor of oriented macromolecules in the absence of structural information. *J. Magn. Reson.* **133**, 216-221.
22. Devries, L., Mousli, M., Wurmser, A. & Farquhar, M.G. (1995). GAIP, a protein that specifically interacts with the trimeric G-protein G-alpha(I3), is a member of a protein family with a highly conserved core domain. *Proc. Natl Acad. Sci. USA* **92**, 11916-11920.
23. de Alba, E., De Vries, L., Farquhar, M. & Tjandra, N. (1999). Solution structure of human GAIP (Gα interacting protein), a regulator of G protein signaling. *J. Mol. Biol.* **291**, 927-939.
24. Starich, M.R., Wikstrom, M., Arst, H.N., Clore, G.M. & Gronenborn, A.M. (1998). The solution structure of a fungal AREA protein–DNA complex: an alternative binding mode for the basic carboxyl tail of GATA factors. *J. Mol. Biol.* **277**, 605-620.
25. Gruschus, J.M., Tsao, D.H.H., Wang, L.H., Nirenberg, M. & Ferretti, J.A. (1999). The three-dimensional structure of the vnd/NK-2 homeodomain–DNA complex by NMR spectroscopy. *J. Mol. Biol.* **289**, 529-545.
26 Kay, L.E. & Gardner, K.H. (1997). Solution NMR spectroscopy beyond 25 kDa. *Curr. Opin. Struct. Biol.* **7**, 722-731.
27. Koradi, R., Billeter, M. & Wüthrich, K. (1996). MOLMOL: a program for display and analysis of macromolecular structures. *J. Mol. Graph.* **14**, 51-55.